Automated 3D extraction of hydromorphological metrics from LiDAR data

Alexandre Rétat[1], Nathalie Thommeret[2], Frédéric Gob[3], Jean-Stéphane Bailly[4], Laurent Lespez[5], Karl Kreutzenberger[6], Thomas Depret[7]

[1] Université Paris-Est Créteil, Laboratoire de Géographie Physique, CNRS UMR 8591 – alexandre.retat@cnrs.fr
[2] Université Paris-Est Créteil, Laboratoire de Géographie Physique, CNRS UMR 8591 - nathalie.thommeret@u-pec.fr
[3] Université Paris 1 Panthéon-Sorbonne, Laboratoire de Géographie Physique, CNRS UMR 8591 - frederic.gob@univ-paris1.fr
[4] LISAH, Univ. Montpellier, AgroParisTech, INRAE, Institut Agro, IRD, Montpellier, France - bailly@agroparistech.fr
[5] Université Paris-Est Créteil, Laboratoire de Géographie Physique, CNRS UMR 8591 - laurent.lespez@u-pec.fr and laurent.lespez@cnrs.fr
[6] Office français de la biodiversité, Direction générale, Service Eau et Milieux Aquatiques - karl.kreutzenberger@ofb.gouv.fr
[7] Laboratoire de Géographie Physique, CNRS UMR 8591, Université Paris-Est Créteil, Université Paris 1 Panthéon-Sorbonne – thomas.depret@cnrs.fr

Keywords: LiDAR, Point cloud, Hydromorphology, Bankfull width, Hydraulic geometry

Abstract

Hydromorphological characterization is essential for understanding river functioning, ecological status, and sediment dynamics, particularly in the context of large-scale environmental monitoring programs such as the European Water Framework Directive. The increasing availability of high-density national LiDAR datasets offers new opportunities for automated and standardized river analysis. This paper presents an automated framework for extracting hydromorphological metrics from LiDAR point clouds, combining two complementary methods: *RiverCourse*, dedicated to river centerline delineation using a Random Forest model applied to pre-classified point clouds, and *Bf3D*, which estimates bankfull elevation and width through a reach-scale three-dimensional hydraulic depth analysis. Unlike conventional cross-section-based approaches, the methodology operates directly in 3D, reducing sensitivity to transect placement and local topographic variability. Applied to 1,440 river reaches from the French Carhyce database, *RiverCourse* achieved an 88% acceptable delineation rate, demonstrating strong robustness across a wide range of river morphologies. The main limitations were associated with low ground-point density under dense vegetation and classification errors affecting bridges or narrow streams. *Bf3D* produced bankfull width estimates in good agreement with field measurements, with a mean percentage deviation of 15.7%. Results also indicate that method performance is strongly dependent on centerline quality and is particularly effective in alluvial systems, while confined rivers remain more challenging due to the absence of clear floodplain signatures. Overall, the framework demonstrates the potential of national LiDAR datasets for automated, standardized, and large-scale hydromorphological assessment.

1. Introduction

Hydromorphological characterization is a key component of river system assessment, providing fundamental indicators of channel geometry, sediment regime, and riparian structure. In Europe, the Water Framework Directive requires member states to achieve at least a “good ecological status” for all water bodies, such status being partly controlled by the degree of hydromorphological alteration. Within this framework, the French national Carhyce program (Hydromorphological Characterization of French Rivers) has been collecting field-based hydromorphological measurements at monitoring river reaches since 2009 (Gob et al., 2025). This field dataset includes data such as channel bankfull width, slope, sediment size, and riparian vegetation. However, the field approach is subject to significant logistical and methodological constraints. Consequently, the hydromorphological assessment is based on a sample of representative contexts of the overall status of water bodies, and large-scale implementation across the whole of France remains difficult to carry out. Meanwhile, the national LiDAR HD program led by IGN (French National Institute of Geography) now provides a homogeneous and high-density 3D dataset covering the entire French territory, except French Guyana. This unprecedented data availability creates an opportunity to automate the extraction of hydromorphological metrics over very large spatial extents. In this context, we developed an automated 3D methodology to extract bankfull parameters, comprising two steps: *RiverCourse*, which is designed to draw the relevant centerline, and *Bf3D*, which computes a detrended DTM with flattened watercourse to extract the bankfull stage and width. Both steps use pre-classified LiDAR point clouds. The bankfull level corresponds to the level at which the channel begins to flood the floodplain. This paper presents the methodology, its validation against the Carhyce database, and its potential for large-scale hydromorphological assessment.

2. Method and data

The entire methodology is divided into two steps. The *RiverCourse* method uses 3D pre-classified point clouds and a Random Forest model to predict the flow direction iteratively from an upstream point, drawing a river centerline as it does so. Then, the *Bf3D* method uses the centerline and a digital terrain model (DTM) to extract bankfull elevation and width.

2.1 Study Sites

The study focuses on 1,440 river reaches in metropolitan France, long of 15 times their bankfull width, taken from the Carhyce database (Figure 1). The river's hydromorphological characteristics, such as width, longitudinal slope and sinuosity, reveal a wide range of river reach typologies. This allows the results of the method to be analyzed in relation to these data.

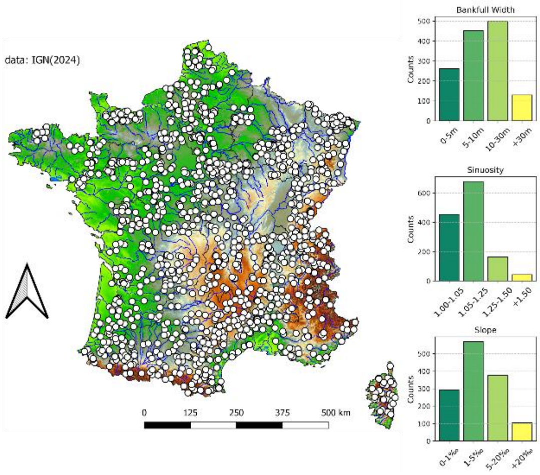

Figure 1: (left) Location of study reaches in Metropolitan France; (right) Histograms of study reaches characteristics taken from Carhyce database. a) Bankfull width; b) Sinuosity; c) Longitudinal slope

2.2 Extraction of the water surface centerline

Widely-used methods for extracting hydrographic networks from DTMs rely on flow-direction and flow accumulation calculation (O’Callaghan and Mark, 1984; Jenson and Domingue, 1988). These methods are particularly effective for large-scale mapping of hydrographic networks due to the simplicity of their calculations. However, they have limitations regarding the accuracy of the initial data, the choice of thresholds, and the presence of complex anthropogenic structures (Charleux-Demargne & Puech, 2000; Thommeret et al., 2010; Datta et al., 2022). Moreover, these methods extract valley bottom and not centerline of a riverbed. The watercourses most affected by these limitations are small streams, where frequent riparian vegetation can distort the data (Christensen et al., 2022). Nevertheless, these small watercourses make up the vast majority of the river network. Those between 0- and 5-meters wide account for 82.28% of the river network in French metropolitan areas (BD Topo, IGN) and are essential for maintaining biodiversity, moving sediment, and regulating water chemistry (Alexander et al., 2007; MacDonald & Coe, 2007; Meyer et al., 2007; Richardson, 2019). This is why studying them, though still very limited compared to larger rivers, is of paramount importance. LiDAR data is now widely used to create high-precision DTM, particularly due to its ability to penetrate vegetation cover. In geomorphology, however, the LiDAR point cloud is often set aside as an intermediate dataset in the process of calculating a raster DTM, because raster maps often adequately meet the need for elevation representation and because point clouds are considered too complex to process and store. However, studying the point cloud reveals interesting elements, such as the spatial distribution of returns in stream vicinity, in light of the interaction between light beams and water. The classification also enables the analysis of features such as the distribution of riparian vegetation. The *RiverCourse* method harnesses this potential for precise delineation at the scale of a watercourse. The method takes as inputs parameter upstream point coordinates P_0 and a rough estimate of the river width W. In each iteration, a new P_i point is computed on the river path in the downstream direction. The next sections describe each step of one iteration, with i the identifier of the iteration.

2.2.1 Points selection

The first step consists to select all the LiDAR points around the P_{i-1} coordinates, in a radius proportional to the rough estimation of width. Then, these points are assigned to a 0.5° sector representing their orientation from P_{i-1} (Figure 2).

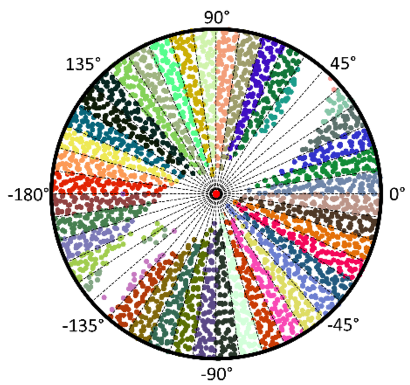

Figure 2: Cloud points sectorization around P_{i-1} (8° sectors instead of 0.5° for visibility)

2.2.2 Calculation of a River Direction Score

The aim of this step is to determine which of these sectors is most likely to represent the direction of flow. To achieve this, a Random Forest model computes a River Direction Score, normalized between 0 and 1, for each sector. The Random Forest model relies on 16 features computed for each sector, along with their mean (μ) and standard deviation (σ) across all sectors. It focuses on three key LiDAR point cloud properties: geometry, point density over water, and classification. In theory, under data optimal conditions, the sector aligned with the river flow at this very local scale should display a nearly negative constant slope, contain no ground or building points, include fewer vegetation points than other sectors, feature multiple water points, and potentially include bridge points. Under optimal conditions, the resulting River Direction Score looks like a double gaussian curve, where maxima correspond to upstream and downstream direction (Figure 3).

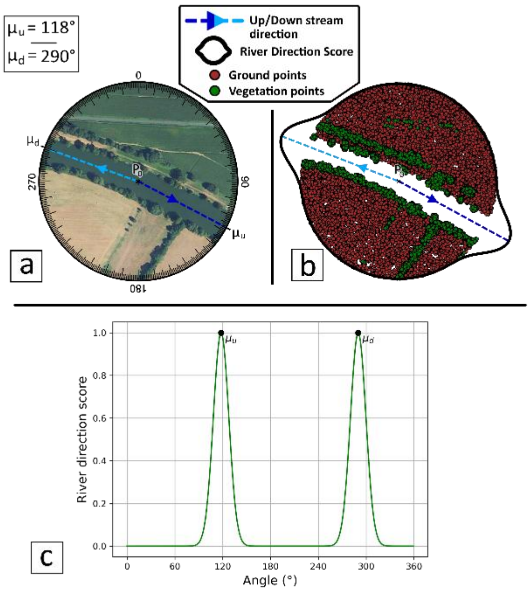

Figure 3: a) Orthophotos of the Loir River reach with manually determined upstream orientation ($\mu_u = 118°$) and downstream orientation ($\mu_d = 290°$); b) LiDAR point cloud with theoretical river direction scores as black line; c) Theoretical River Direction Score function.

2.3 Identification of bankfull stage

Previous studies (McKean et al., 2009; De Rosa et al., 2019; Garber et al., 2024) have demonstrated that bankfull metrics can be semi-automatically extracted from high-resolution regular DTMs at the cross-section scale, and then averaged at the reach scale. However, these methods present several major limitations: (i) dependence on manually defined transects and subjective cross-section placement, (ii) high sensitivity to micro-topographic noise and local variability, and (iii) limited generalization across different channel types and scales. Our approach, *Bf3D*, addresses these issues by replacing the traditional 2D transect-based framework with a continuous 3D computation, enabling full automation over a wide range of fluvial styles. The challenges that *Bf3D* aims to address are: (i) the construction of a detrended irregular DTM based on a centerline consistent with the LiDAR data, (ii) the translation of the bankfull parameters estimation method, originally based on hydraulic depth on cross-section, into three dimensions, and (iii) the optimization of the scripts to enable automated processing across multiple rivers reaches.

2.3.1 Reconstruction of a flattened irregular DTM

Using the centerline, a DTM is then computed. To minimize information loss due to interpolation, a TIN (Triangulated Irregular Network) mesh is preferred over a raster representation. The DTM and the centerline are subsequently used to calculate the mean slope of the reach and to generate a detrended DTM. The final step involves flattening the water surface, resulting in a DTM in which the water can rise horizontally.

2.3.2 Computation of bankfull width estimate

In line with numerous studies (Williams, 1978; McKean et al., 2009; De Rosa et al., 2019), we use the hydraulic depth (Hd) to estimate the bankfull level of the reach. Since our analysis is conducted in three dimensions, the formula is adapted to express Hd as the ratio between the wetted volume and wetted surface area at successive water levels h raised by 10 cm (Equ. 1):

$$Hd_h[m] = \frac{V_h[m^3]}{S_h[m^2]} \tag{1}$$

The resulting curve can show breakpoints that correspond to significant increases in wetted surface area for a small increase in volume. In theory, these local maxima indicate flooding over flat surfaces, such as floodplains, as well as over bars or terraces. We use the ratio between the hydraulic depth of each local maximum and the subsequent local minimum to determine the most significant flooding, which we associate with that on the floodplain (Figure 4). If there is no maximum, the lowest increase in hydraulic depth is associated with the bankfull stage.

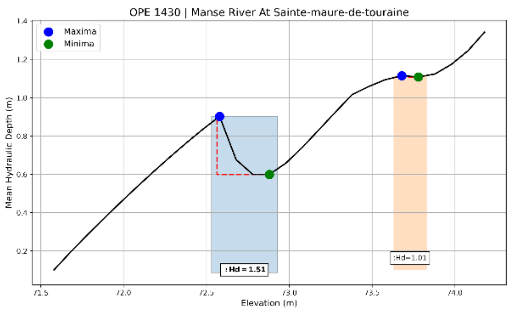

Figure 4: Hydraulic depth curve of the Manse River reach function of elevation. Two maxima corresponding to two flood stages have been identified; the first is considered the floodplain stage.

Once the bankfull level is determined, the corresponding width is calculated as the quotient of the surface area at bankfull level and the length of the reach. This approach integrates the entire topographic surface of the reach, thereby avoiding the bias induced by transect orientation and spatial discretization.

2.4 Quality assessment

2.4.1 *RiverCourse* quality assessment

The quality of the *RiverCourse* delineation results was achieved through a four-class qualitative assessment. This assessment was based on observations of LiDAR data, mapping of point altitudes and densities, and ortho-photography where possible. The four classes are designed as follows:

1 - High: The vast majority of vertices are considered to be centered.

2 – Good: Some vertices are not centered but are still located within the riverbed.

3 – Moderate: The line follows the trend, but not always within the riverbed.

4 – Bad: The vertices are increasingly distant from the riverbed.

The pre-expectation assumes that only classes 1 and 2 are considered acceptable for hydromorphological calculations.

2.4.2 *Bf3D* quality assessment

Thanks to the Carhyce database, we have a dataset of bankfull widths measured on the field. The time between field and LiDAR acquisitions may be several years. We analyze the *Bf3D* results using the Absolute Percentage Deviation (APD) indicator (Equ. 2) in relation to the Carhyce database.

$$APD = 100 \times \left| \frac{W_{Bf}^{Bf3D} - W_{Bf}^{Carhyce}}{W_{Bf}^{Bf3D}} \right| \quad (2)$$

2.5 The LiDAR HD data

The data used in this study comes from the LiDAR HD program, which is led by the French National Institute of Geography (IGN). It is a nationwide coverage of France (except French Guyana) using high-density topographic LiDAR, i.e. a minimum of 10 pulses per square meter are emitted. The Point clouds are given in projection Lambert93/IGN69 (EPSG 2154) with a precision controlled to obtain a $EMQ_{EN} \leq 25cm$ and $EMQ_{H} \leq 5cm$ in relative (IGN, 2023). The classification respects the ASPRS specification including ground, water, bridge, building, vegetation (low, medium and high). A hybrid approach combining deterministic methods, external data, and probabilistic deep learning techniques have been applied to make the classification (Gaydon, 2022; Pauthonnier, 2024).

3. Results

3.1 Centerline assessment

Of the 1,440 river reaches, 64.58% are classified as Class 1, and the overall acceptance rate (Classes 1 and 2 combined) is 88.02%. Class 3 represents 7.22% of the total. To ensure relevant results, the remaining river reaches whose centerline was classified as Class 4 were excluded from the Bf3D computation.

3.2 Main delineation error sources

The Table 1 summarizes the four main factors that may lead to errors in the *RiverCourse* results. Note that these factors, determined visually from the manual assessment, do not always result in errors; only instances where errors were observed are reported, i.e. for river reaches in classes 2, 3 and 4. Moreover, several errors can occur at a single reach. We used the Cochran–Armitage test to assess monotonic trends of each error type across classes. The Z-value indicates the direction and strength of the trend (positive toward poorer classes, negative toward better ones), while the p-value reflects its statistical significance. The "Mean Class" corresponds to the average class of affected reaches.

The first factor identified was the low ground point density, particularly under vegetation cover (LD). This is due to the absorption of LiDAR beams by vegetation. This effect varies greatly at the scale of the programme because it depends on the nature of the vegetation, the acquisition period, meteorological conditions, etc. The second factor is that the *RiverCourse* method tends to clip the meanders at their concave parts (MC). This often causes a deviation from the real centreline, but rarely results in the centreline leaving the minor bed. The last two sources of error are due to classification. The presence of points on the water surface is rare, and the classification process uses exogenous data to classify them as "water". For narrower rivers, which are not well described in the national dataset, the classification process often fails and classifies them as 'ground' (WG). The same errors cause points on bridges to be classified as ground (BG).

As shown in Table 1, MC and WG display negative trends, whereas LD and BG show positive trends. The presence of ground-classified points on water (WG) is not significant (p = 0.2881), indicating a weak effect rather than a sample size issue; this is supported by manual checks showing limited impact on classification. In contrast, high sinuosity (MC) shows a significant negative trend (Z = -4.215), generally maintaining classifications within acceptable ranges. Vegetation-induced lack of ground points (LD) exhibits a strong positive trend and is a major cause of poor classifications, particularly in Class 4 cases. Similarly, bridge points classified as ground (BG) contribute to deviations, with a consistent impact across classes indicating a clear limitation of the model.

Observed error	Frequency			Statistical metrics		
	Class 2	Class 3	Class 4	Mean Class	Z	p-value
Low ground points density (LD)	162	66	41	2.55	3.597	6e-4
Meander clipped (MC)	115	18	0	2.14	-4.215	1e-4
Water points classified as ground (WG)	121	38	9	2.33	-1.461	0.288
Bridge points classified as ground (BG)	16	13	12	2.90	3.643	5e-4

Table 1: Results of the Cochran-Armitage test on the four main error sources from the *RiverCourse* method.

3.3 Number of maxima on hydraulic depth curves

A major source of potential error in the *Bf3D* method is selecting the wrong maxima corresponding to flooding. This can occur in the presence of bars or terraces whose surface is much higher than that of the flooding. A poor delineation, especially when the line leaves the riverbed, also causes the risk of that the wrong area is flattened, which can cause irrelevant flooding and therefore a false maximum on the hydraulic depth curve. It is therefore interesting to observe the number of maxima present in the *Bf3D* results (Figure 5). The first thing to note is that the majority of hydraulic depth curves (70.7%) have only one maximum. 16.6% of the reaches do not present maximum and can correspond to confined rivers where there is no floodplain to be determined. For reaches presenting several maxima, it can correspond for example to braided stream, rivers with multi-terraces in their alluvial plain, reaches close to human-built plan structure or errors in DTM flattening process due to incorrect delineation.

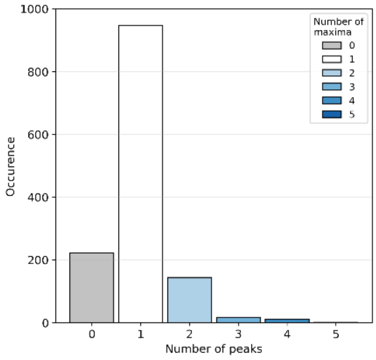

Figure 5: Histogram of number of maxima on the full dataset of hydraulic depth curves.

3.4 Comparison between Carhyce and Bf3D bankfull width

The comparison between Carhyce bankfull widths and *Bf3D* generally yields good results (Figure 6), despite a global overevaluation by *Bf3D*, with a Mean Percentage Deviation of 15.72%. The average APD is 37.54% for the total reaches. It decreases to 31.43% when conserving only reaches presenting a unique maximum on their hydraulic depth curve. Reaches that do not show a maximum on their hydraulic depth curve have an average APD of 45.56%, further underscoring the irrelevance of *Bf3D* for confined rivers.

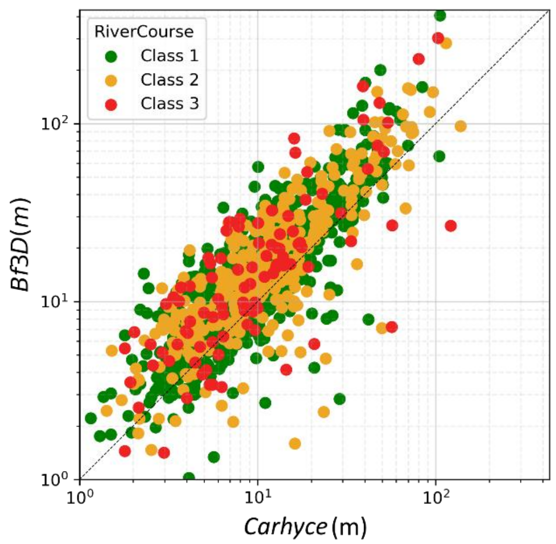

Figure 6: Comparison of bankfull width between Carhyce database and Bf3D, colored by *RiverCourse* assessment results.

3.5 Impact of *RiverCourse* on *Bf3D* results

Figure 7 clearly shows the impact of the delineation on the quality of the *Bf3D* methodology. The median APD rises from 25.6% for Class 1, to 37.6% for Class 2, to 42.5% for Class 3. It confirms the necessity and value of precise delineation for hydromorphological analyses, such as *Bf3D*.

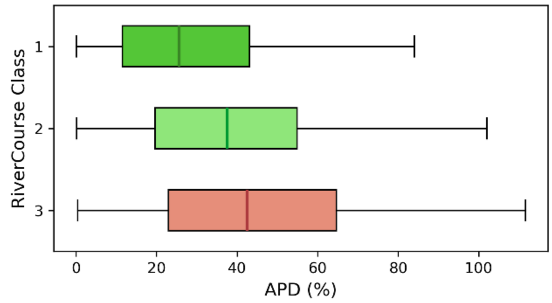

Figure 7: Box and whisker plots (lower quartile, median, upper quartile values) of the Absolute Percentage Deviation, function of reach *RiverClass* assessment.

3.6 Relationship between *Bf3D* results and hydromorphological characteristics

The analysis of the APD depending on reaches hydromorphological characteristics seems to reveal an improvement of the results when sinuosity rises and slope decreases but it's not very clear concerning bankfull width (Figure 8). A high factor limiting the quality of *Bf3D* are the non-alluvial river reaches. These confined river reaches, often presenting a slightly straight channel and a significant slope, do not present a clear floodplain. Therefore, the use of *Bf3D* is already of little relevance, and its result can't be good.

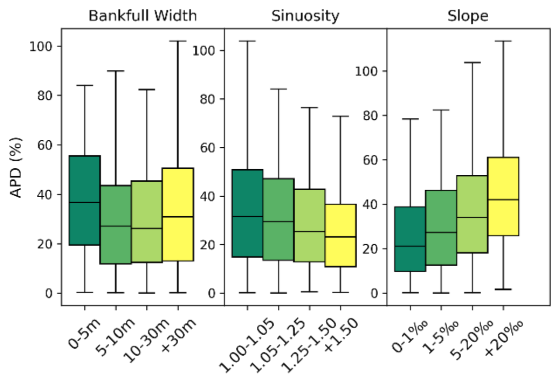

Figure 8: Box and whisker plots (lower quartile, median, upper quartile values) of the Absolute Percentage Deviation, function of reach bankfull width, sinuosity and slope.

4. Discussion and Conclusion

These results demonstrate that accurate bankfull measurements are possible, provided the watercourse is accurately located. In the vast majority of cases, *RiverCourse* can fulfill this role. Compared with traditional methods based on flow accumulation, which enables rapid extraction of entire hydrographic networks, the *RiverCourse* approach is not designed to compete at large spatial scales. Instead, it focuses on detailed, local analyses at the scale of individual watercourses. By combining elevation with point density and classification, *RiverCourse* achieves highly precise delineation of watercourses, whereas flow accumulation methods depend exclusively on elevation data. This level of precision is particularly valuable for both cross-sectional and longitudinal studies, where delineation is often performed manually in the field or through photo interpretation. Such manual processes can be time-consuming and labor-intensive, especially for small streams located beneath forest cover. The results indicate that *RiverCourse* is more sensitive to data quality than to intrinsic river characteristics, particularly regarding point density under vegetation. The features of the Random Forest model allow the method to be applied to virtually any LiDAR point cloud. While ground classification remains essential, and can be done for example through Cloth Simulation algorithm, additional classes such as water, vegetation, and bridges significantly improve algorithm performance without being mandatory. Although this study focuses on reach-scale analysis to ensure robust evaluation across varying hydromorphological conditions and LiDAR datasets, the method can be extended to longer river sections. However, a key limitation is the potential for the algorithm to deviate from the true channel path. One way to improve robustness is to first perform a coarse pre-delineation using a larger window size, which can guide the algorithm and constrain excessive deviations. Accurate bridge classification is also critical; if unavailable, external datasets such as bridge geodata should be incorporated.

Since *Bf3D* requires accurate delineation of the watercourse, the centerlines processed by RiverCourse provide a good starting point. The *Bf3D* methodology is difficult to assess since the only available reference bankfull width dataset at this scale is Carhyce, an assessment on the ground. Because the use of 3D data instead of cross-section represents another perception of bankfull, the Carhyce dataset is certainly an excellent dataset for comparison purposes, but it cannot be considered as a truth reference that the *Bf3D* method wishes to reach. Nevertheless, comparison of their data still shows a good correlation between the two approaches. Tested in a large quantity of reaches presenting a wide range of slope, width and sinuosity values, *Bf3D* proved that it can be applied to both large and small rivers. It performs particularly well in alluvial systems, enabling automated and robust hydromorphological measurements. However, it is less suited to confined rivers and can struggle in environments where multiple flat surfaces are adjacent to the channel. With further refinement, *Bf3D* could support near-exhaustive characterization of fluvial landscapes at large scales while maintaining consistency across results. Ongoing work aims to extend its application to longer river segments. From a methodological perspective, *Bf3D* represents a significant shift in hydromorphological analysis. It moves away from discrete, cross-section-based approaches toward a continuous 3D framework, enabling fully automated computation of channel metrics at the reach scale. This approach also supports reproducibility at national scales within standardized workflows. Overall, *Bf3D* demonstrates that hydromorphological indicators can be derived automatically and consistently from high-density national LiDAR datasets, with accuracy approaching that of field-based measurements. Future research will aim to expand this capability from localized reach-scale studies to continuous, catchment-wide analyses.

References

Alexander, R. B., Boyer, E. W., Smith, R. A., Schwarz, G.E., Moore, R. B., (2007). The Role of Headwater Streams in Downstream Water Quality. *JAWRA Journal of the American Water Resources Association, 43(1)*, 41-59. https://doi.org/10.1111/j.1752-1688.2007.00005.x

Charleux-Demargne, J., Puech, C., (2000). Quality assessment for drainage networks and watershed boundaries extraction from a digital elevation model (DEM). *GIS '00: Proceedings of the 8th ACM international symposium on Advances in geographic information systems*, 89-94. https://doi.org/10.1145/355274.355287

Christensen, J. R., Golden, H. E., Alexander, L. C., Pickard, B. R., Fritz, K. M., Lane, C. R., Weber, M. H., Kwok, R. M., Keefer, M. N., (2022). Headwater streams and inland wetlands: Status and advancements of geospatial datasets and maps across the United States. *Earth-Science Reviews, 235*, 104230. https://doi.org/10.1016/j.earscirev.2022.104230

Datta, S., Karmakar, S., Mezbahuddin, S., Hossain, M. M., Chaudhary, B. S., Hoque, M. E., Abdullah Al Mamun, M. M., Baul, T. K., (2022). The limits of watershed delineation: implications of different DEMs, DEM resolutions, and area threshold values. *Hydrology Research, 53(8)*, 1047-1062. https://doi.org/10.2166/nh.2022.126

De Rosa, P., Fredduzzi, A., Cencetti, C., (2019). A GIS-Based Tool for Automatic Bankfull Detection from Airborne High Resolution Dem. *ISPRS International Journal of Geo-Information*, 8(11), 480. https://doi.org/10.3390/ijgi8110480

Garber, J., Thompson, K., Burns, M.J., Kunapo, J., Zhang, G.Z., Russel, K., (2024). Artificial intelligence and objective-function methods can identify bankfull river channel extents. *Water Resources Research*, 60. https://doi.org/10.1029/2023WR035269

Gaydon, C., (2022). Myria3D: Deep Learning for the Semantic Segmentation of Aerial Lidar Point Clouds. *IGN (French Mapping Agency)*.

Gob, F., Thommeret, N., Bilodeau, C., Tamisier, V., Rivière, R., Kreutzenberger, K., (2025). Assessing the morphological alteration of river reaches from 15 years of measurements: French hydromorphological database and indicators (Carhyce). *Geomorphology*, 479, 109737. https://doi.org/10.1016/j.geomorph.2025.109737

IGN, (2023). LiDAR HD - Version 1.0 - Descriptif du contenu des nuages de points LiDAR.

Jenson, S. K., Domingue, J.O., (1988). Extracting topographic structure from digital elevation data for geographic information-system analysis. *Photogrammetric Engineering and Remote Sensing, 54(11)*, 1593-1600.

MacDonald, L. H., Coe, D., (2007). Influence of Headwater Streams on Downstream Reaches in Forested

Areas. *Forest Science, 53(2)*, 148-168. https://doi.org/10.1093/forestscience/53.2.148

Mckean, J., Nagel, D., Tonina, D., Bailey, P., Wright, C.W., Bohn, C., Nayegandhi, A., (2009). Remote Sensing of Channels and Riparian Zones with a Narrow-Beam Aquatic-Terrestrial LIDAR. *Remote Sensing*, 1(4), 1065-1096. https://doi.org/10.3390/rs1041065

Meyer, J. L., Strayer, D. L., Wallace, J. B., Eggert, S. L., Helfman, G. S., Leonard, N. E., (2007). The Contribution of Headwater Streams to Biodiversity in River Networks. *JAWRA Journal of the American Water Resources Association, 43(1)*, 86-103. https://doi.org/10.1111/j.1752-1688.2007.00008.x

O'Callaghan, J. F., Mark, D. M., (1984). The extraction of drainage networks from digital elevation data. *Computer Vision, Graphics, and Image Processing, 28(3)*, 323-344. https://doi.org/10.1016/s0734-189x(84)80011-0

Pauthonnier, A., (2024). Le Programme Lidar HD de l'IGN. Forum de la Topographie 2024, *Association Francophone de Topographie*.

Richardson, J. S., (2019). Biological Diversity in Headwater Streams. *Water, 11(2)*, 366. https://doi.org/10.3390/w11020366

Thommeret, N., Bailly, J. S., Puech, C., (2010). Extraction of thalweg networks from DTMs: application to badlands. *Hydrology and Earth System Sciences*, *14*(8), 1527-1536. https://doi.org/10.5194/hess-14-1527-2010

Williams, G.P., (1978). Bank-Full Discharge of Rivers. *Water Resources Research*, 14(6), 1141-1154. https://doi.org/10.1029/WR014i006p01141